International Journal of Minerals, Metallurgy and Materials
Volume 27, Number 9, September 2020, Page 1165
https://doi.org/10.1007/s12613-020-2004-5

Invited Review

Mechanics and safety issues in tailing-based backfill: A review

Xu Zhao[1)], *Andy Fourie*[1)], *and Chong-chong Qi*[2)]

1) School of Civil, Environmental and Mining Engineering, University of Western Australia, Perth 6009, Australia
2) School of Resources and Safety Engineering, Central South University, Changsha 410083, China
(Received: 17 October 2019; revised: 2 February 2020; accepted: 10 February 2020)

Abstract: Voids (referred to as "stopes") are generally created during underground mining activities and can lead to both local and regional geotechnical instabilities. To assist in managing the stability of mining-related voids and improving the recovery of orebodies, tailing-based backfill technology has been widely used around the world. In the design of tailing-based backfill strategy, the specific function and engineering requirements of the filling are intimately dependent on the stress distribution within the backfilled stope. In this paper, the main mechanics involved in tailing-based backfill in underground mines, which include arching, consolidation, hydration process, and movement of surrounding rocks, are reviewed. Research on the safety of a barricade and stability of an exposed fill face are also presented. In conclusion, the backfilling process should be performed on the basis of a better understanding of the complicated interactions of the mechanisms of filling, consolidation, and hydration process (when cement is added).

Keywords: tailing-based backfill; arching; consolidation; barricade; safety

1. Introduction

Extracting valuable minerals from the earth's crust is the essence of mining [1]. Mining activities generally result in the creation of voids. Referred to as stopes, these voids vary in size but can be as large as 30 m × 30 m in plan dimensions and more than 100 m tall, leading to various environmental impacts, such as ground surface settlement on both local and regional scales [2–3]. To maintain geotechnical stability, significant pillars of valuable ore must be left between stopes, which can significantly reduce the quantity of ore recovered [4].

To assist in managing the stability of mining-related voids and improving the recovery of orebodies, backfilling has been widely used in many mined stopes [5–6]. The types of fill applied and their specific functions and engineering requirements are intimately dependent on the mining methods, mining strategies, and mining sequences.

The main types of mine backfilling include hydraulic fill, in which high-density slurry is delivered through boreholes and pipelines to the underground workings; paste backfill, which is generated from full-stream tailings and is now a widely accepted alternative means of mine backfilling; and rock fill, which economically uses waste rock generated from mining operations as the main component of the fill material.

This paper mainly focuses on tailing-based backfill, which includes both hydraulic fill and paste backfill. A key advantage of tailing-based backfill is its capability to transport the material hydraulically. Given this characteristic, the material handling and delivery costs of tailing-based backfill are relatively low, whereas the establishment of the stress state in a tailing-based backfill is complicated because of the existence of water [7]. In cases where cement is added to the backfill material, attempts to characterize the behavior of the fill during deposition and subsequent hydration become even more complicated [8–10].

Fig. 1 schematically shows the backfilling system in a stope. At the bottom of the stope, an access tunnel (also called "drawpoint") is connected to the stope for the recovery and removal of blasted ore. To enable filling of the stope, at a certain location along the access tunnel, a containment barricade is constructed to prevent the fill from flowing out of the stope during and after backfilling.

In the design of the backfill strategy, the stress state in the backfilled stope should be controlled such that it does not present a risk to workers underground, e.g., if the full hydraulic head within a stope is imposed on a barricade, it can result in rupture of the barricade, potentially causing an underground mud rush. This needs to be avoided at all costs, as it presents a serious risk to workers. However, limited know-

Corresponding author: Chong-chong Qi E-mail: chongchong.qi@csu.edu.cn

ledge of the unexpected behavior of the fill can result in catastrophic consequences, such as the failure of containment barricades or the failure of a fill mass during exposure. Therefore, more insights into the stress distribution within the backfilled stope are required to ensure the safety of tailing-based backfill systems.

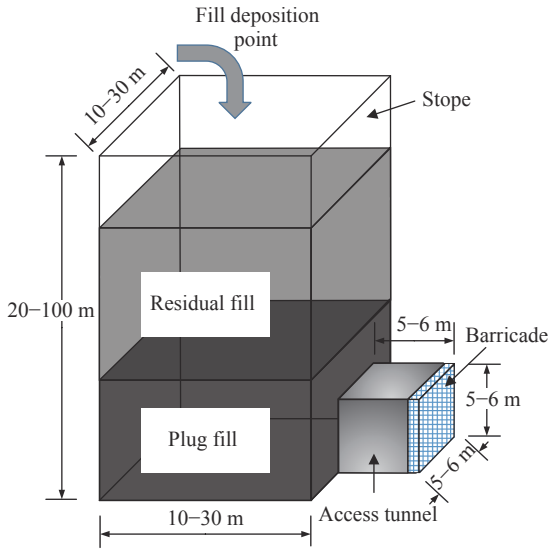

Fig. 1. Schematic of a typical layout in a backfilled stope.

This paper presents an overview of the literature relevant to the mechanics and safety issues in the mine backfilling process. First, the non-geostatic stress state of "arching" in mine backfilling is discussed. Then, consolidation theory and cement hydration, the methodologies of fully coupling these mechanisms, and the influence of the behavior of surrounding rock mass are addressed. Finally, previous approaches used to analyze the stability of an exposed fill face and the safety of a barricade are presented. For a detailed discussion about the properties of the backfill body from the materials science point of view, interested readers can refer to the companion review paper from the same group [11].

2. Arching theory

In industry, the backfilling process is mainly divided into two steps, namely, plug filling and residual filling. To monitor the stresses developed within the backfill or behind the backfill barricades, some *in situ* monitoring operations were conducted, where stress sensors were placed within the stope [12–13]. In these monitoring programs, the initial stress monitored by the bottom sensor increases with the filling operation, which is closely related to the self-weight stress or consolidation loads. However, after plug filling, the measured stress slightly decreases. After residual filling, the measured stress at the bottom exhibits a gradual increase, and the increase rate is lower than the expected increase rate of the self-weight stress. This means that the total stress induced by the overlying backfill body was mainly transferred to the surrounding rock, and many scholars attribute this phenomenon to the mechanism known as "arching" [14–17]. The essence of arching within the backfilled stope is load transfer along the wall/fill interfaces induced by the shear forces. Notably, the "arching" in the backfilled stope is one of most important concepts adopted in this paper because it may have a significant impact on the stress state in the stope, thereby leading to safety issues in the exposed vertical face and barricade of the access tunnel. As a starting point, this section provides an overview of existing methodologies to investigate the arching phenomenon and highlights a number of areas where further research can improve the understanding of this phenomenon.

The concept of stress arching has been discussed by many different researchers over the years, including the pioneering works of Janssen [18], Marston [19], and Terzaghi [20]. In recent years, this theory has been applied to the development of limit state solutions specific to the mine backfilling situation [14,21–23].

Marston [19] provided a specific analytical solution for estimating the arching effect on a backfilled mine stope, which takes into account the shearing forces along the fill/rock interfaces. Fig. 2 shows the different force components of the backfilled mine stope.

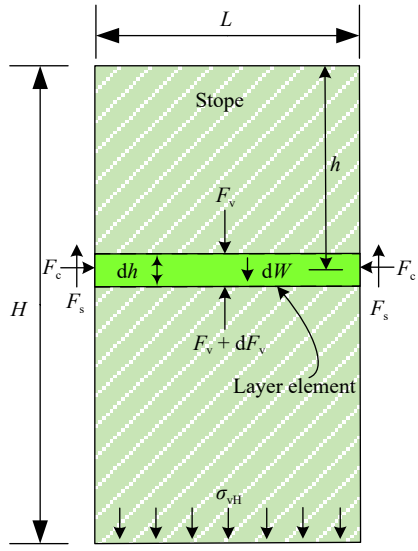

Fig. 2. Schematic of the forces acting on a typical vertical backfilled stope.

As shown in Fig. 2, L and H are defined as the width and height of the backfilled stope, respectively. A horizontal layer element (at position h) is subjected to vertical compressive forces F_v and $F_v + dF_v$, a shearing force F_s, and a horizontal compressive force F_c. dW is the self-weight of the layer and dh is the thickness of the layer. The average vertical stress at the bottom (σ_{vH}) is expressed as follows:

$$\sigma_{vH} = (\gamma L - 2c)\frac{1-\exp(-2KH\tan\delta/L)}{2K\tan\delta} \quad (1)$$

where γ is the bulk unit weight of the fill, K is the earth pressure coefficient, c is the cohesion of the backfill, and δ is the interfacial friction angle.

Some useful modifications have also been made on the basis of this solution to adapt to wide geometric boundaries and external mechanical conditions. For example, Li and Aubertin [24] extended the analytical solution for "fully drained" conditions to consider "hydrostatic" conditions, as follows:

$$\sigma_{vH} = ((\gamma_{sat} - \gamma_w)L - 2c)\frac{1-\exp(-2KH\tan\delta/L)}{2K\tan\delta} + u_w \quad (2)$$

where γ_{sat} and γ_w are unit weights of the saturated fill and water, respectively, and u_w is the water pressure under hydrostatic equilibrium.

Rajeev *et al.* [25] and Widisinghe [26] extended the analytical expression of total stress to a three-dimensional scenario, such as that of a cylinder, as follows:

$$\sigma_{Hv} = (\gamma_{sat} - \gamma_w)L\frac{1-\exp(-4KH\tan\delta/L)}{4K\tan\delta} + u_w \quad (3)$$

where L is converted into the diameter of the cylinder.

The calculated vertical stress of the analytical solution expressed in Eq. (1) is highly dependent on the interfacial friction angle δ and the earth pressure coefficient K. For Marston's theory, three values of K have been considered [27].

(1) Pressure at rest, K_0:

$$K_0 = 1 - \sin\phi \quad (4)$$

(2) Active pressure, K_a:

$$K_a = \tan^2\left(45° - \frac{\phi}{2}\right) \quad (5)$$

(3) Passive pressure, K_p:

$$K_p = (1 + \sin\phi)/(1 - \sin\phi) \quad (6)$$

where ϕ is the friction angle of the fill material. Different values of K (K_0 or K_a) have been used in previous researches [14–28].

The expressions of Marston's theory [19] and the extended theory are a useful and fast methodology for the preliminary evaluation of stress distribution under some specific and simplified conditions. However, as with the limit equilibrium method, this method has the following internal limitations: (1) It always assumes the full mobilization of shearing stress at the fill/rock interfaces [16]. (2) It ignores the fundamental properties of cemented backfill that evolve with time, as well as the possibility of material yield at the fill/rock interfaces when large deformation occurs. (3) It assumes a constant value for Rankine's earth pressure coefficient, although investigations clearly show that this coefficient tends to vary with the location of a backfilled opening [15,29].

In conclusion, the previously mentioned investigations found that, even under "fully drained" conditions, the degree of arching is determined by the complicated interaction between the mechanical properties of the fill. The behavior of the fill is more complicated under "undrained" or "partially drained" conditions when the mechanism of consolidation is involved. As will be shown in the following section, neglecting pore pressure in the calculation of the stress distribution can lead to a gross oversimplification of the process.

3. Consolidation behavior of the fill

This section presents the current research on the complicated interactions between the mechanism of stress arching and the consolidation process during filling placement and curing.

Fourie *et al.* [30] explained the significance of effective stress to the analysis of the behavior of the fill. The adjective "effective" is used to indicate that it is this stress, and not the total stress, that dictates the strength and stiffness of uncemented soils; furthermore, it is this effective stress that produces the deformation of the soil "skeleton." Therefore, a thorough understanding of the mechanism of stress redistribution to the surrounding rock mass is constructed on the basis of the understanding of the effective stress. To understand effective stress, an understanding of the consolidation process is required.

3.1. Numerical consolidation analysis

Many numerical investigations have been conducted to demonstrate the significance of consolidation on the arching phenomenon in the fill mass [15,17,26,31].

Fahey *et al.* [15] undertook a series of numerical simulations using a commercial code (Plaxis 2D), where the Mohr–Coulomb constitutive model was chosen. In their study, a stope with the height of 50 m and width of 20 m was modeled. To determine the effect of consolidation on the stress state, as well as the arching mechanism, they divided these cases into either fully drained or saturated conditions: (1) The fully drained case neglected the influence of pore water pressure; thus, it can be considered a valid representation of the "best case scenario." Assuming that the water table had been drawn to the bottom of the stope quickly and atmospheric pressures existed throughout most of the fill mass, the importance of elastic parameters was investigated. (2) In a fully saturated backfill, the investigation was focused on the differences in stress state (i.e., effective stress, total stress, and water pressure) in the stope at the end of filling (EOF), at the end of consolidation process (EOC), and at the end of water table drawdown (EOD).

The corresponding curves of stresses in three cases (i.e., A, B, and C) that assumed a fully drained situation are reproduced in Fig. 3. The material properties adopted in this analysis included the bulk unit weight of 20 kN/m^3, Poisson's ratio (ν) of 0.2, Young's modulus (E) of 10 MPa, angle of

dilation (ψ) of 10°, and angle of friction (ϕ) of 45°. Case A presented a plane strain stope with the width of 20 m, and case C showed an axisymmetric stope with the diameter of 20 m. The stress distribution within a stope with the width of 10 m (case B), which is only half that of case A, was also investigated. To demonstrate the influence of the arching theory, the overburden of fill without arching is shown in Fig. 3 denoted by a dashed line.

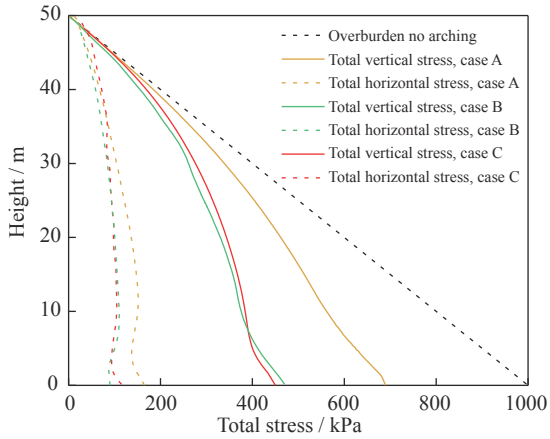

Fig. 3. Vertical and horizontal stresses in three cases, that is, fully drained (based on the study of Fahey *et al.* [15]).

As shown in Fig. 3, the vertical stresses in the three cases are lower than the overburden weight because of the arching effect. The effect of the width of the stope is also clear: The arching effect is significant when the stope is narrow, which is consistent with the conclusion of the analytical approach of Marston's theory in Section 2.

Some interesting results for drained filling were also provided: (1) Poisson's ratio (ν) is important in modeling because it determines the values of the constrained modulus (M) and shear modulus (G). (2) When the fill becomes incompressible ($\nu \rightarrow 0.5$), there is insufficient settlement of the fill to mobilize the shear force at the fill/rock interfaces; hence, no arching would occur. (3) Compared with the plane strain model, the axisymmetric model has shown more arching effect. The main reason is that the two-dimensional model could not represent the three-dimensional arching (termed "doming") in the axisymmetric case.

Notably, in the lower 5 m of the stope, there are different degrees of steeper increase in total vertical stress. This phenomenon has also been observed in other works [32–33]. This finding can be attributed to the reduction of settlement toward the stiff base of the stope. Thus, less shear strain is mobilized at the interface. As a result, less stress redistribution or "arching" occurs toward the base.

Apart from the results of "drained" cases, the most important aspect of the research of Fahey *et al.* [15] is the investigation of the significance of consolidation on the overall arching development.

Fig. 4 shows the curves of the total horizontal and vertical stresses at three stages of the filling process, namely, EOF, EOC, and EOD. The water table was initially set at the top during consolidation and then drawn down to the base. The material properties used are the same as those in the "fully drained" case. Moreover, effective cohesion c' is 0 and permeability k is 1×10^{-3} m/d.

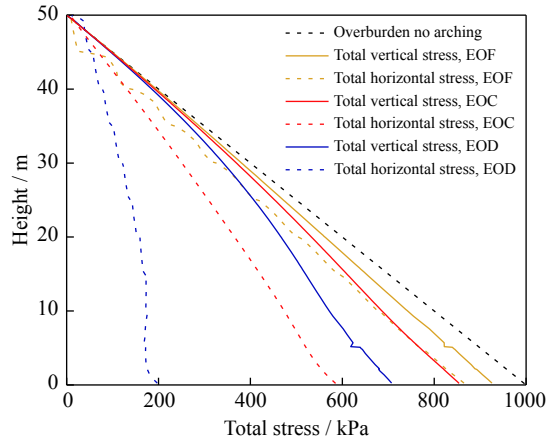

Fig. 4. Undrained filling: total vertical and horizontal stresses at EOF, EOC, and EOD (based on the study of Fahey *et al.* [15]).

At EOF, the total horizontal and vertical stresses were almost equal to the overburden stress; this situation is called "almost undrained." If the backfill strategy is applied to the stope, where the filling rate is quick and the permeability of the fill material is low, then the "almost undrained" or even "completely undrained situation" may occur.

As explained in Section 2, to mobilize any shear stress at the fill/rock interfaces, shear strains are required. To generate shear strain, the material must settle. However, under "almost undrained" conditions, the compressive stiffness of the bulk material is that of water, which is high. Thus, only slight settlement occurs. If all of the self-weight stresses are supported by the water phase, then the total horizontal stress will be equal to the total vertical stress. It is not until water is squeezed out of the fill mass that soil compression (settlement) can occur and shear strains at the interface can occur, generating the "arching" effect. With the progress of consolidation, the vertical stress decreases and the horizontal stress becomes obviously lower than the vertical stress at the same depth (curves at EOC).

At EOD, the stress was further reduced, reaching the "fully drained" state. Notably, in the study of Fahey *et al.* [15], permeability was assumed to remain constant. However, in practice, permeability will decrease with the compression of the backfill.

The study of Fahey *et al.* [15] derived an important conclusion: The arching can only develop within a backfilled stope with the progress of consolidation because of the shear stress in the fill/rock interfaces that is induced by the com-

bined effects of the settlement of the fill and development of effective stress. This conclusion is verified by *in situ* monitoring projects [12]: Hydrostatic loading at the bottom of a stope was measured for more than 20 h, and the results indicated that no arching occurred in the early filling stage, after which the backfilling operation was stopped and the measured pressures decreased with the progress of consolidation.

3.2. Analytical consolidation modeling

Gibson [34] proposed an analytical expression for the calculation of consolidation in a deposit of saturated soil where the thickness of the deposit increases with time. The derived solution is a relationship between the development of excess pore pressure (u_{ex}), the coefficient of consolidation (c_v), the current thickness of the deposit ($h(t)$), and the time that filling has been ongoing (t) in a one-dimensional situation (x is the elevation above the base), as follows:

$$c_v \frac{\partial^2 u_{ex}}{\partial^2 x^2} = \frac{\partial u_{ex}}{\partial t} - \frac{\partial h}{\partial t} \tag{7}$$

The Gibson theory is well suited to the case of paste backfill and hydraulic fill placement into the stope. Notably, both permeable and impermeable boundary conditions at the base were analyzed by Gibson [34]. In most cases, the floor stratum of rock is often considered impermeable, whereas the barricade constructed at the end of the drawpoint is considered free draining (although this is often not ensured in practice). Moreover, the flow area of the drawpoint is often significantly smaller than that of the stope. As a result, it may be more appropriate to ultimately assume an impermeable condition at the base.

Another point that might be argued is that the one-dimensional solution cannot strictly describe the behavior of the fill in a stope, as it neglects the potential effect of arching between rock and fill. Therefore, Gibson's theory can provide a reasonable representation of the consolidation process in the early stage of placement when arching has not occurred [15].

4. Cementation hydration process of cemented-tailing-based backfill

When cement is added to the fill and the cement particles undergo hydration, a number of chemical reactions occur. These reactions result in the growth of hydrates that effectively act to connect the particles. The hydration process of cement has a significant influence on the strength, consolidation, and many other characteristics of backfill behavior [35–39]. Notably, the current review paper focuses on the mechanics of cemented-tailing-based backfill. In contrast to investigations from the materials science point of view, the mechanical behavior of cemented-tailing-based backfill has not been well investigated. Some variables (i.e., binder type and dosage) that influence the backfill properties are considered and simplified in the investigation of its mechanical behavior. For a detailed discussion about the backfill properties, readers can refer to the paper of Qi and Fourie [11]. In the following sections, an overall picture of the cementation hydration process of cemented-tailing-based backfill is provided from the mechanics point of view.

4.1. Maturity of the hydration process

During the placement of cemented backfill, the material initially behaves in accordance with the characteristics of uncemented material. However, as cement hydrates, the behavior of the material changes. To represent the cementation process, the maturity functions used in previous research are reviewed in this section.

Illston *et al.* [40] simulated the rate of hydration of the four main compounds that make up cement paste. Their work indicated that the individual compounds react at vastly different rates.

Other researchers have developed empirical relationships to represent the rate of hydration of the overall cement product [37,41]. These authors call the rate of hydration "maturity" and essentially fit various curves to the development of cement-related characteristics (maturity) against time.

The exponential relationship proposed by Rastrup [41] was adopted to represent the maturity of cement throughout this paper. This simple exponential relationship between cement hydration and time can be expressed as follows:

$$m = \exp\left(\frac{-d}{\sqrt{t^*}}\right) \tag{8}$$

where m is the maturity degree (from 0 at the beginning to 1 at the end of the chemical reaction); d is a constant, $d^{\frac{1}{2}}$; and t^* is the time since the initial set t_0, d.

Investigations, which will be presented later in this paper, indicate that the rates of change of strength, stiffness, permeability, and volume due to the hydration process can all be appropriately represented using the same maturity relationship.

4.2. Mechanism of "self-desiccation"

The mechanism of "self-desiccation" has been well documented with respect to its significant influence on the behavior of tailing-based backfill [2,37,42].

The essence of the "self-desiccation" process is that net volume loss will occur after the hydration reaction. Prior to cement hydration, per unit volume of cemented backfill is assumed to contain a certain volume of cement (V_{cu}). After the hydration process, the increased volume of cement is expressed as $\Delta V_{hyd} = V_{ch} - V_{cu}$, where V_{ch} is the volume of hydrated cement. However, the increased volume ΔV_{hyd} is less than the volume of used water (V_{wh}) in this process. Therefore, the total loss of volume in this enclosed system is denoted as ΔV_{sh} (the "chemical shrinkage" volume).

Helinski *et al.* [37] proposed the following analytical

model for the incremental change in pore pressure (Δu) and shrinkage volume (ΔV_{sh}) using the principles of stress equilibrium and strain compatibility:

$$\Delta u = -\frac{\Delta V_{sh}}{V_w V_T}\frac{K_w K_s}{(K_s/V_T + K_w/V_w)} = -\frac{\Delta V_{sh}}{V_T}\frac{K_w}{(n + K_w/V_s)} \quad (9)$$

where V_T represents the total volume of the combination of water and soil, V_w represents the total volume of the pore water, K_w and K_s represent the stiffnesses of water and soil, respectively, and n represents the porosity of the fill.

In conventional concrete masses, the water content is relatively lean. To derive the expression of shrinkage volume (ΔV_{sh}, cm^3), Powers and Brownyard [43] experimentally determined the relationship between ΔV_{sh} and the mass of chemically combined water (W_n, g) for a cement paste in a fully hydrated system:

$$\Delta V_{sh} = 0.279 W_n \quad (10)$$

Empirically, the mass of cement contained in most General Portland cements is $W_n = 0.23 W_c$, where W_c is the mass of unhydrated cement. Therefore, the empirical expression for the shrinkage volume and original mass of cement is as follows:

$$\Delta V_{sh} = 0.064 W_c \quad (11)$$

It should be noted that this empirical expression applies only to General Portland cements. For each particular ratio of cement and tailings, the variable E_h can be adopted [37]:

$$\Delta V_{sh} = E_h W_c \quad (12)$$

In combination with the "maturity model" for cement hydration (Eq. (8)), Helinski *et al.* [37] proposed an expression to represent the volume of chemical shrinkage at a given time (t). Then, the rate of change of water volume was derived as follows:

$$\frac{\delta(\Delta V_{sh})}{\delta t} = -\frac{1}{2}E_h W_c \left(\frac{d}{(t^*)^{1.5}}\right)\exp\left(\frac{-d}{\sqrt{t^*}}\right) \quad (13)$$

Walske [44] compared the chemical shrinkage determined using Eq. (13) with that measured in laboratory tests. Their results indicated that, with the fitted values of E_h and W_c, Eq. (13) can favorably represent the experimental chemical shrinkage data.

Notably, different from conventional concrete masses, tailing-based backfill slurries typically have higher initial water content and lower cement content. Thus, only a small portion of water will be involved in the hydration process. Despite this, these volume changes still have a significant influence on the pore pressure changes and the stress state in the backfill [2].

4.3. Coupled analysis model of the cemented backfilling process

4.3.1. One-dimensional consolidation and hydration modeling

Gibson *et al.* [45] derived the large-strain consolidation equation by combining the equilibrium of the soil and water phases using Darcy's law to represent flow. By combining these equations and maintaining continuity, they derived the following governing equation to represent the one-dimensional large-strain consolidation of uncemented slurry:

$$\underbrace{\frac{\delta u}{\delta t}}_{(A)} + \underbrace{\left\{(1+e_0)\frac{\delta \sigma'_v}{\delta e}\right\}}_{(B)}\underbrace{\left\{\frac{\delta}{\delta \beta}\left[\frac{k}{\gamma_w}\left(\frac{1+e_0}{1+e}\right)\frac{\delta u}{\delta \beta}\right] + \frac{\delta k}{\delta \beta}\right\}}_{(C)} = \underbrace{\frac{\delta \sigma_v}{\delta t}}_{(D)} \quad (14)$$

where σ_v and σ'_v are total and effective vertical stress, respectively, e_0 is the initial void ratio, e is the void ratio at time t, β is a Lagrangian coordinate, and k is the permeability. Term D represents the rate of application of total stress, which results in the rate of reduction of pore pressure (term A); term C is the volumetric strain, which contains the current permeability of the fill; and term B is the current stiffness of the fill.

In cemented backfill, the impacts associated with cement hydration, which include the development of cement-induced stiffness and strength, the reduction in permeability, and the mechanism of "self-desiccation," need to be considered. Therefore, Helinski [33] modified a constitutive equation that considers the impacts of the hydration process to obtain the following expression:

$$\underbrace{\left\{\frac{\delta u}{\delta t}\left[1 - \frac{e}{K_w}\frac{\delta \sigma'_v}{\delta e}(t, C_c, e, \sigma'_v)\right]\right\}}_{(A)} + \underbrace{\left\{\frac{\delta \sigma'_v}{\delta e}(t, C_c, e, \sigma'_v)(1+e_0)\right\}}_{(B)}\underbrace{\left\{\frac{\delta}{\delta e}\left[\frac{k(e_{eff})}{\gamma_w}\left(\frac{1+e_0}{1+e}\right)\frac{\delta u}{\delta \alpha}\right] + \frac{\delta k(e_{eff})}{\delta \alpha}\right\}}_{(C)} + \underbrace{\left\{\frac{\delta \sigma'_v}{\delta e}(t, C_c, e, \sigma'_v)\frac{\delta V_{sh}(t, C_c)}{\delta t}\right\}}_{(E)} = \underbrace{\frac{\delta \sigma_v}{\delta t}}_{(D)} \quad (15)$$

where e_{eff} represents the effective void ratio. The terms correspond to the relevant terms in Eq. (14). Term A (the change in pore pressure) accounts for K_w and the matrix stiffness ($\delta \sigma'_v / \delta e$), which depends on the void ratio (e), cement content (C_c), and vertical effective stress (σ'_v). In term C (volumetric strain), k is dictated by the effective void ratio (e_{eff}), which is influenced by the cement gel developed in the void. Term E accounts for the volumetric change V_{sh} associated with the mechanism of "self-desiccation."

Helinski *et al.* [46] incorporated the constitutive model described previously into a finite element program (CeMinTaCo) to conduct a full analysis of cemented backfill.

4.3.2. Coupled consolidation and hydration analysis with the finite element numerical program

Helinski [33] developed a plane strain finite element numerical program (called "Minefill-2D") to predict the behavior of cemented backfill. The program has been verified to provide an accurate prediction of the behavior of the fill within the backfilled stope [47]. Furthermore, being a self-developed program, the Minefill-2D exhibits unique scalability and evolution capability. The description of the governing equations and numerical formulations developed and material models adopted in the Minefill-2D program are presented in this section.

(1) Governing equations.

In cemented filling, once the time reaches t_0, the cement hydration process begins to influence the material behavior. Thus, the cement hydration process should be coupled with the consolidation process. According to Helinski [33], the influence of the hydration process is most significantly associated with the following parameters: (1) Stiffness. The density of the fill, evolution of cement hydration, and damage to the cement bonds caused by excessive strain can influence the stiffness of the fill, which is reflected in the time-evolved constitutive matrix $[D']$, and therefore, the global stiffness matrix $[K_G]$. (2) Strength. The strength of the fill is influenced by cement hydration, as well as by the destruction of cement bonds due to excessive stress, as indicated by the change of the constitutive matrix $[D']$ and the global stiffness matrix $[K_G]$. (3) Permeability. The permeability matrix $[\Phi_G]$ interacts with material density, particle size distribution, and cement hydrate growth. (4) Self-desiccation. This refers to the volume changes that occur during the hydration process and can be taken into account through the internal sink term Q.

To take account of the cement hydration process during the consolidation process, the functions of time, material state (void ratio), and cement content should be incorporated into the relevant terms of the governing consolidation equation, as follows:

$$\begin{bmatrix} [K_G(t,e,C_c)] & [L_G] \\ [L_G]^T & -\Delta t[\Phi_G(t,e,C_c)] \end{bmatrix} \begin{bmatrix} \{\Delta d\}_{nG} \\ \{\Delta u\}_{nG} \end{bmatrix} = \begin{bmatrix} \{\Delta R_G\} \\ ([n_G(t,e,C_c)] + Q(t,e,C_c) + [\Phi_G(t,e,C_c)]\{u\}_{nG})\Delta t \end{bmatrix} \tag{16}$$

where $[L_G]$ is volume matrix, $[n_G]$ is flow due to gravitational forces, $\{\Delta R_G\}$ is the change of boundary stresses, $\{\Delta d\}_{nG}$ is the vector of displacement increments, and $\{\Delta u\}_{nG}$ is the vector of total pore pressure increments.

The behavior of both uncemented and cemented fill materials and the numerical models used to characterize such behavior adopted in Minefill-2D are discussed in the following sections.

(2) Strength and stiffness, $[K_G(t,e,C_c)]$.

According to Helinski [33], a power law has been successfully applied to the compression behavior of uncemented mine tailings. Hence, this function was adopted to relate the void ratio to the applied effective stress, taking the following form:

$$e = a_c(\sigma')^{b_c} \tag{17}$$

where σ' is the mean effective stress and a_c and b_c are curve-fitting constants.

By differentiating Eq. (17) and combining the result with well-known elastic relationships, the uncemented shear stiffness $G_{(uncem)}$ can be derived as follows:

$$G_{(uncem)} = \frac{\partial\sigma}{\partial e}\frac{(e+1)}{2(1+\nu)} = \frac{(e+1)}{2a_cb_c(1+\nu)}\left(\frac{e}{a_c}\right)^{(1/b_c-1)} \tag{18}$$

The Mohr–Coulomb failure criterion is applied as the material model in Minefill-2D, where the size of the yield surface is governed by the state of the material and hydration degree [2]. The shear stiffness is dependent on the mobilized stress and the size of the yield surface.

In cemented filling, the cohesive strength increases as a result of cement hydration and decreases due to damage caused by yield stress, which can be expressed as follows:

$$\partial c' = \frac{\partial \mathrm{Hyd}}{\partial t} - \frac{\partial D}{\partial \varepsilon_S^P} \tag{19}$$

where $\partial c'$ is the change in the effective cohesion, $\partial \mathrm{Hyd}/\partial t$ is the change of c' with time due to hydration, and $\partial D/\partial \varepsilon_S^P$ is the degradation of c' with time due to plastic shear strain ($\partial \varepsilon_S^P$).

In Minefill-2D, the rate of development of cohesion with time can be expressed as follows:

$$\frac{\partial c'}{\partial t} = \frac{1}{2}\left(\frac{d}{(t^*)^{1.5}}\right)\exp\left(\frac{-d}{\sqrt{t^*}}\right)A_c\exp\left(\frac{XC_c + C_c^{0.1} - e}{ZC_c + W}\right) \tag{20}$$

where A_c, X, Z, and W are curve-fitting constants and C_c is the cement content.

If the material is strained beyond yield, then progressive breakdown of the bond strength can occur. This mechanism has been accounted for by reducing c' linearly as a function of the plastic shear strain ε_S^P (i.e., the $\partial D/\partial \varepsilon_S^P$ term in Eq. (19)).

The cement-induced component of stiffness is assumed to be linearly related to c, with a constant friction angle. This assumption is convenient for modeling in Minefill-2D: By evolving the cohesive intercept in accordance with Eq. (20), the cement-induced component of stiffness can be linearly related to this value in accordance with a constant rigidity term.

To represent the pre-yield response, a nonlinear stiffness function was adopted. This function degrades the material tangential stiffness linearly as the shear stress approaches yield in accordance with the following equation:

$$G_{t(cem)} = G_{0(cem)}\left[1 - f\left(\frac{\tau_{mob}}{\tau_{max}}\right)\right] \tag{21}$$

where τ_{mob} is the mobilized shear stress, τ_{max} is the yield

stress, $G_{t(\mathrm{cem})}$ is the contribution of cement to the tangential shear stiffness, $G_{0(\mathrm{cem})}$ is the cement component of the small strain shear stiffness, and f is a curve-fitting constant. The actual value of f can be experimentally derived from a triaxial stress–strain curve.

(3) Permeability, $[\Phi_{\mathrm{G}}(t,e,C_{\mathrm{c}})]$, $[n_{\mathrm{G}}(t,e,C_{\mathrm{c}})]$.

Permeability can have a significant influence on the overall consolidation behavior. As shown in Eq. (16), $[\Phi_{\mathrm{G}}]$ represents the permeability submatrix.

In uncemented filling or before the initial set time t_0 in cemented filling, the void volume of the fill reduces with compression, which can lead to a reduction in permeability. Carrier *et al.* [48] developed a relationship that has been shown to provide a good representation of the relationship between void ratio and permeability of fill materials. This function was adopted in Minefill-2D, as follows:

$$k = \frac{c_{\mathrm{p}}(e)^{d_{\mathrm{p}}}}{1+e} \tag{22}$$

where c_{p} and d_{p} are constants.

To account for the growth of cement solids, the void ratio term e in Eq. (22) is modified to be the effective void ratio (e_{eff}). Therefore, the permeability function is modified to derive the following expression:

$$k = \frac{c_{\mathrm{p}}(e_{\mathrm{eff}})^{d_{\mathrm{p}}}}{1+e} \tag{23}$$

(4) Self-desiccation, $Q(t,e,C_{\mathrm{c}})$

The mechanism of "self-desiccation" has a significant effect on the overall behavior of cemented-tailing-based backfill [38]. This relationship was implemented in Minefill-2D as an internal sink term and expressed as follows:

$$Q(t,e,C_{\mathrm{c}}) = -\frac{1}{2}E_{\mathrm{h}}W_{\mathrm{c}}\left(\frac{d}{(t^*)^{1.5}}\right)\exp\left(\frac{-d}{\sqrt{t^*}}\right) \tag{24}$$

The rate of hydration (d) and hydration efficiency (E_{h}) are fundamental properties of the fill and can be obtained experimentally with each cement and tailings combination.

4.3.3. Multiphysics modeling

The coupled multiphysics analysis is well documented in the literature on cemented backfill [49–51]. Among these studies, Cui and Fall [42] proposed a thermo–hydro-mechanical–chemical (THMC) model to conduct a fully coupled analysis of cemented backfill.

$$nS\frac{\partial \rho_{\mathrm{w}}}{\partial t} + n\rho_{\mathrm{w}}\frac{\partial S}{\partial t} + S\rho_{\mathrm{w}}\left(\frac{\partial \varepsilon_{\mathrm{v}}}{\partial t} + \frac{(1-n)}{\rho_{\mathrm{s}}}\frac{\partial \rho_{\mathrm{s}}}{\partial t}\right) - nSm_{\mathrm{hydr}} = -\nabla(nS\rho_{\mathrm{w}}v^{\mathrm{rw}}) \tag{25}$$

$$n(1-S)\frac{\partial \rho_{\mathrm{a}}}{\partial t} - n\rho_{\mathrm{a}}\frac{\partial S}{\partial t} + (1-S)\rho_{\mathrm{a}}\left(\frac{\partial \varepsilon_{\mathrm{v}}}{\partial t} + \frac{(1-n)}{\rho_{\mathrm{s}}}\frac{\partial \rho_{\mathrm{s}}}{\partial t} - \frac{nS}{\rho_{\mathrm{s}}}m_{\mathrm{hydr}}\right) = -\nabla n(1-S)\rho_{\mathrm{a}}v^{\mathrm{ra}} \tag{26}$$

$$\nabla\left(\frac{\partial \sigma}{\partial t}\right) + \frac{\partial((1-n)\rho_{\mathrm{s}} + nS\rho_{\mathrm{w}} + n(1-n)\rho_{\mathrm{a}})}{\partial t}g = 0 \tag{27}$$

$$((1-n)\rho_{\mathrm{s}}C_{\mathrm{s}} + nS\rho_{\mathrm{w}}C_{\mathrm{w}} + n(1-S)\rho_{\mathrm{a}}C_{\mathrm{a}})\left(\frac{\partial T}{\partial t}\right) + Q_{\mathrm{ad}} + Q_{\mathrm{cd}} = Q_{\mathrm{hydr}} \tag{28}$$

where S is the saturation degree; ρ_{a}, ρ_{w}, and ρ_{s} represent the densities of air, water, and solid, respectively; ε_{v} is the volumetric strain; m_{hydr} is the reduction rate of water volume in the hydration process; v^{rw} and v^{ra} are the apparent velocities of water and air in the fill, respectively; g is the acceleration of gravity; C_{a}, C_{w}, and C_{s} represent the specific heat capacities of air, water, and solid, respectively; Q_{ad} and Q_{cd} represent the advection and conduction heat transfer, respectively; and Q_{hydr} is the generated heat due to the chemical reaction.

The proposed model was implemented in the commercial finite element program COMSOL. This coupled analysis has been validated against laboratory and *in situ* measured data. Furthermore, an evolutive elastoplastic model has been incorparated to consider the interaction between fill and rock mass [52].

A detailed comparison of existing works on coupled analysis described previously is provided in Table 1.

5. Influence of the deformation and movement of surrounding rock mass

The previous sections have discussed the research on the stress state in a backfilled stope with a rigid boundary condition. However, the influence of the deformation and movement of surrounding rock mass has not yet been thoroughly investigated [53].

Falaknaz *et al.* [53] verified that the stress state in a stope can be significantly influnced by the excavation of the neighboring stopes. However, an anomalous stress increase within the fill mass undisturbed by mining operations has been captured in some *in situ* monitoring projects [13,54–55]. The unexpected increase of stress reduces the consistency of the predicted and measured behavior of the fill, thus compromising the stability of the fill mass and retaining structures. For example, for 80 d, more than 100 kPa of increasing stresses was recorded by Thompson *et al.* [13] in the absence of any further filling.

The reason for the anomalous stress increase has been discussed extensively. Thompson *et al.* [12] arributed this phenomenon to the temperature increase casued by the hydration of cement. However, in a monitoring program conducted in Australia, a similar stress increase was also observed, but with only a measured temperature increase of 6°C [54], indicating that other factors may cause the anomalous stress increase. Fig. 5 shows the measurement of the anomalous stress increase in a backfilled stope [56].

Qi and Fourie [56] proposed that this anomalous stress in-

Table 1. Summary and comparison of existing works on coupled analysis of cemented-tailing-based backfill

Coupled analysis	Mechanical model	Program	Remarks	Source
One-dimensional consolidation and hydration analysis	Structured Cam Clay model	Self-developed finite element program (CeMinTaCo)	(1) Incorporate a large-strain formulation; (2) Take account of cement hydration; (3) Account for development of a partially saturated matrix.	[46]
Two-dimensional consolidation analysis	Mohr-Coulomb model	Self-developed finite element program (Minefill-2D)	(1) Capture the strain and chemical hardening behavior; (2) Incorporate the "arching" mechanism; (3) Incorporate a self-desiccation model; (4) Account for water accumulation above the fill surface; (5) Strain softening of the fill mass due to interface shear during filling.	[2]
Three-dimensional THMC multi-physics analysis	Evolutive elastoplastic model	Commercial finite element program (COMSOL)	(1) Capture the strain hardening/softening behaviour; (2) Consider mechanical behavior of the fill and walls; (3) Incorporate a self-desiccation model; (4) Consider the thermal deformation (expansion or contraction); (5) Varies mixture recipe and curing condition on binder hydration.	[38]

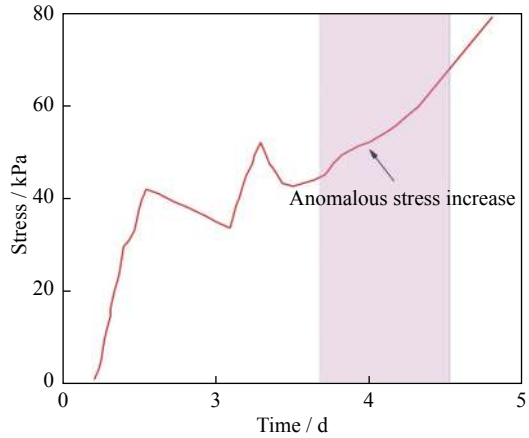

Fig. 5. Measurement of the anomalous stress increase. Adapted from Qi and Fourie [56].

crease is closely related to the movement of surrounding rock mass. Although the surrounding rock mass of a backfilled stope has been considered in previous studies [2,29], it has been invariably represented as a rigid boundary. However, the influence of the behavior of surrouding rock on the fill mass is a time-dependent process. Therefore, Qi and Fourie [56] incorporated the creep behavior of the rock mass (CBRM) of the stope and demonstrated the influence of the time-dependent deformation of the rock mass on the stress distribution within the stope.

The constitutive laws can be expressed as follows:

$$\begin{cases} \dot{e}_{\mathrm{v}} = \dot{e}_{\mathrm{v}}^{\mathrm{e}} + \dot{e}_{\mathrm{v}}^{\mathrm{P}} \\ \dot{e}_{ij} = \dot{e}_{ij}^{\mathrm{K}} + \dot{e}_{ij}^{\mathrm{M}} + \dot{e}_{ij}^{\mathrm{P}} \end{cases} \tag{29}$$

where $\dot{e}^{\mathrm{K}}$, $\dot{e}^{\mathrm{M}}$, $\dot{e}^{\mathrm{P}}$, and $\dot{e}^{\mathrm{e}}$ are the Kelvin, Maxwell, plastic, and elastic strains, respectively, and $\dot{e}_{ij}$ and $\dot{e}_{\mathrm{v}}$ are deviatoric and volumetric components, respectively.

In addition, the relationships between viscoelastic components can be expressed as follows:

$$\begin{cases} \text{Kelvin: } s_{ij} = 2\eta^{\mathrm{K}}\dot{e}_{ij}^{\mathrm{K}} + 2G^{\mathrm{K}}e_{ij}^{\mathrm{K}} \\ \text{Maxwell: } \dot{e}_{ij}^{\mathrm{M}} = \dfrac{\dot{s}_{ij}}{2G^{\mathrm{M}}} + \dfrac{s_{ij}}{2\eta^{\mathrm{M}}} \end{cases} \tag{30}$$

where s_{ij} is the deviatoric component, G^{K} and G^{M} are the Kelvin and Maxwell shear moduli, respectively, and η^{K} and η^{M} are the Kelvin and Maxwell viscosities, respectively.

A plane strain stope was modeled with the finite element code FLAC to estimate the interaction between the fill mass and the CBRM in backfilled stopes. Its consistency with the engineering applications indicates that the proposed model can potentially explain the anomalous stress increase during the backfilling process.

Notably, in practice, after the stope is created, there is often a rest time before starting the filling operations. Thus, the main convergence of surrounding walls was assumed to have finished during this period and the rock walls are assumed to be rigid and totally fixed. However, this is definitely an interesting topic that could be investigated in future works, particularly in mines where the deformation of rock strata or the disturbance from nearby mining operations is significant.

6. Strength of the cemented-tailing-based backfill and stability of the exposed fill face

6.1. Analytical solutions of the stability of the exposed fill face

When adjacent stopes are extracted, the confining stress is

reduced, which in turn reduces the stability of the fill mass and imposes the need for the exposed fill faces to become self-supporting (as shown in Fig. 6 [57]). If the fill mass has insufficient cohesive strength, then fill failure can occur, resulting in the dilution of the ore being mined in the adjacent stope. Therefore, a critical safety issue in the backfilling system is the evaluation of the stability of an exposed backfill face [5].

The traditional solution requires that the unconfined compressive strength (UCS) of the fill be more than the maximum overburden weight in the stope and is expressed as follows:

$$[\sigma]_{\mathrm{UCS}} \geq \gamma H \tag{31}$$

where $[\sigma]_{\mathrm{UCS}}$ is the required UCS.

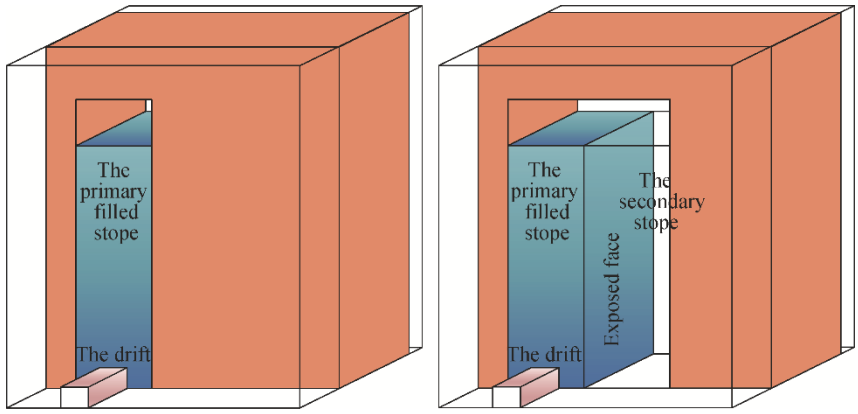

Fig. 6. Schematic of the creation of the vertical exposed fill face in a typical backfilling scenario. Reprinted by permission from Springer Nature: *Int. J. Miner. Metall. Mater.*, An analytical solution for evaluating the safety of an exposed face in a paste backfill stope incorporating the arching phenomenon, X. Zhao, A. Fourie, and C.C. Qi, Copyright 2019.

If the shear forces between the fill/rock interfaces are not considered, then the traditional solution may result in a conservative design of the backfill strategy [58].

In practice, Mitchell's solution is widely used to predict the stability of an exposed fill face [59]. This solution analyzes the stress equilibrium of the potential sliding fill mass and takes account of the shearing effects between backfill and surrounding rocks (Fig. 7 [57]).

According to the model of Mitchell's solution (Fig. 7), the safety factor (F) can be expressed as follows:

$$F = \frac{W_{\mathrm{n}}\cos\alpha\tan\phi + cLB/\cos\alpha}{W_{\mathrm{n}}\sin\alpha} = \frac{\tan\phi}{\tan\alpha} + \frac{2cL}{H^{*}(\gamma L - 2c_{\mathrm{b}})\sin(2\alpha)} \tag{32}$$

where ϕ and c are the internal friction angle and apparent cohesive strength of the backfill, respectively; α represents the angle of the potential sliding plane, taken as $45^{\circ}+\phi/2$; $H^{*}=H-(B\tan\alpha)/2$ is the equivalent height of the wedge block; B represents the length of the stope; and c_{b} is the adhesion strength along the fill/rock interfaces.

A number of useful modifications have been proposed on the basis of this solution [58,60–62]. Some interesting points discussed here are what the contact strength between the fill/rock interfaces could be and how it may be influenced by other mechanisms. In the expression derived by Mitchell *et al.* [59], the interface is cohesive and its contact strength (adhesion strength c_{b}) is equal to that of the fill. Therefore, before estimating the stability of the exposed fill face, predicting the shear behavior of the fill/rock interfaces and the cohesive strength of the fill is important.

Zhao *et al.* [57] proposed a three-dimensional solution to evaluate the safety of an exposed fill face, which is based on Morgenstern's method [63] and the modified differential slice method [64]. For a vertical face of exposed paste backfill, this solution divides the entire wedge block of fill into differential vertical slices, considering the arching effect.

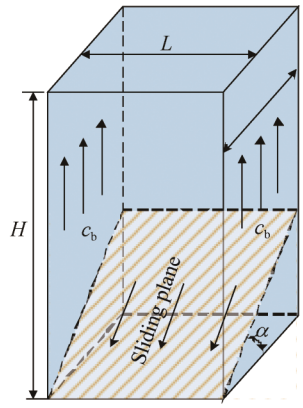

Fig. 7. Confined wedge block model of Mitchell's solution. Reprinted by permission from Springer Nature: *Int. J. Miner. Metall. Mater.*, An analytical solution for evaluating the safety of an exposed face in a paste backfill stope incorporating the arching phenomenon, X. Zhao, A. Fourie, and C.C. Qi, Copyright 2019.

This solution is also suitable for the nonuniform distribution of cohesive strength.

6.2. Factors influncing the strength of the fill

During the filling process, the development of shear strength is dependent not only on material properties [65] but also on other mechanisms, such as boundary conditions, filling rate, and consolidation [33,66]. Many tests have been conducted to evaluate the shear characteristics of the fill [67–70]. In addition, it has been documented that *in situ* backfill strengths are influenced by settlement and drainage and often significantly greater than those measured in the laboratory [71–72].

Fahey *et al.* [73] pointed out that the cohesive strength of *in situ* cemented backfill is also influenced by the curing (effective) stress acting on the backfill, with the process of consolidation through drainage and the mechanism of "self-desiccation" The final strength of the fill specimen is affected by different stresses applied at different curing stages. Therefore, first, a coupled analysis taking account of the arching, consolidation, and cement hydration mechanisms is required to determine the development of the effective stress acting on the fill; then, the strengths representative of the *in situ* conditions can be obtained using the curing protocols for laboratory specimens proposed by Fahey *et al.* [73].

In conclusion, to improve the understanding of the stability of the exposed fill face, the final properties of mine backfilling need to be determined. To determine the final material properties, a thorough understanding of the interaction of arching, consolidation process, and cement hydration is required.

7. Safety of a barricade

Barricades are constructed across the access tunnel to retain the paste backfill during filling operations and while the fill cures. However, barricade failures still occur in recent years, imposing considerable danger to miners located deep in the mine [46,74–75].

Current research indicates that many of the failures occurred because of the bending failure caused by the large pressures imposed on the barricade by paste backfill [76]. Moreover, the bending of a barricade is directly related to the lateral pressure imposed by the fill in the stope. Generally, barricade displacements are relatively small and these displacements are affected by engineering factors, such as *in situ* global rock mass stresses, barricade construction techniques, and mining activities, resulting in larger displacements than those caused by the fill-generated lateral pressure alone. Consequently, it is difficult to verify the barricade's strength and the pressure induced on the barricade, as well as to provide efficient design guidance for mining operations. To solve these problems, some underground mining operations have implemented instrumentation programs that monitor the backfill-generated pressures and resulting deformation of the barricade. However, knowledge of the damage mechanism of the barricade is still limited in the field of mine backfilling.

To prevent failure, the industry typically designs and builds barricades using conservative filling pressures, which means unnecessary cost for underground mines. In addition, to reduce the pressure applied to the shotcrete barricade, many mines apply the discontinuous paste filling strategy, in which stopes are poured in multiple stages, which causes increased stope cycle times [77]. Therefore, the value of pressure exerted on the barricade and the pressure that the designed barricade can withstand are the prerequisites for a complete and rational methodology for the design of barricades in backfilled stopes [78]. Given the importance of the loading pressure, considerable emphasis has been placed on investigating the pressures exerted on a barricade.

Li and Aubertin [16] presented a three-dimensional analytical solution of horizontal stress imposed on the barricade, which takes into account the interaction between backfill and walls of access drift in a "fully drained" situation. In particular, this solution considers the influence of the drift length on the barricade pressure. This solution was expanded to hydrostatic conditions [79]. The limitations of this solution are the same as those of Marston's theory [19], that is, the influence of the consolidation and hydration processes is ignored, thus resulting in uncertainty of the barricade's safety.

Thompson *et al.* [12] conducted a comprehensive field instrumentation project to obtain *in situ* data in two stopes at the Cayeli Mine in Turkey, where total pressure cells were installed at the barricades. Some interesting phenomena were observed: (1) The stope with low filling rate and high binder content of cemented paste backfill showed a rapid departure from hydrostatic loading, and thus relatively low barricade pressures. (2) Conversely, long hydrostatic loading and high barricade pressures were observed in the stope with high filling rate and low binder content of cemented paste backfill. After plug filling, the backfilling operation was stopped and the pressures decreased, probably because of the consolidation and "self-desiccation" processes. (3) The arching effect was observed, with pressures decreasing significantly with the increasing of the drift length. These observations illustrate the effects of filling rate, cement hydration, and geoconditions (such as height of brows and length of the drift) on the barricade pressures.

Although real-time pressure monitoring of paste backfill barricades could provide useful information, the measured stress of earth pressure cells are typically lower than the true values, called "under-registration" [33]. The degree of under-registration is related to the relative stiffness between the cell and the cemented fill. As hydration proceeds, the stiffness of cemented soil increases significantly; thus, the degree of under-registration in such circumstances could also change.

Therefore, the pressure exerted on the mine backfilling barricades is a complex problem in the mining industry and there is a need for more research in this area. Some pioneering works have shown that a comprehensive investigation of this area should incorporate the consolidation process, the hydration process dominated by "self-desiccation," and the influence of arching [33,47,52].

To date, considerable research has focused on investigating the first question. However, to the author's knowledge, there are only a few studies where a comprehensive safety evaluation of a barricade has been incorporated into the analysis of the mine backfilling process. In the mining industry, an empirically derived value for the maximum barricade loading pressure is 100 kPa, which was developed through experience at a number of sites. These "rules of thumb" can result in a successful outcome; however, the validity of these rules of thumb is still questionable because pressure can and does vary dramatically from one operation to another [1]. Revell and Sainsbury [75] investigated the sensitivity of barricade performance to material and geometric characteristics that were likely to vary in the field. In addition, field instrumentation projects of the deformation of barricades were conducted [12].

Currently, the bending behavior of a shotcrete or concrete barricade subjected to fill pressure has been widely simulated as a two-dimensional beam restrained against axial deformation under uniform pressure [80–81]. Comparisons with the experimental results have shown that the beam model predicts the maximum vertical deflection at the mid-span of reinforced concrete beams well. Thus, this simpler and faster two-dimensional analysis could be performed for a given barricade in lieu of a more complex three-dimensional analysis [81].

In conclusion, a comprehensive safety evaluation of a barricade needs to be incorporated into the analysis of the mine backfilling process. Specifically, the in-depth analysis of barricade safety is suggested as a topic for future research.

8. Conclusions

This paper presented an overview of the literature of the mechanics of and safety issues in tailing-based backfill. On the basis of the findings obtained from the literature, the following conclusions are drawn: (1) The stress distribution within a stope is significantly influenced by the degree of arching that occurs in the stope. (2) The consolidation process during backfill is verified to be essential in attempting to determine the stress distribution within a stope. (3) The cement hydration process can significantly influence the behavior of the fill. All of these mechanisms should be incorporated into the understanding of the tailing-based deposition process. (4) The deformation of rock strata or the disturbance from nearby mining operations may significantly change the stress state in the backfilled stope. (5) The safety of the barricade and exposed fill face is directly related to the stress state in the backfilled stope. Meanwhile, more research efforts should be focused on the strength of the fill and the behavior of the barricade.

As outlined in this paper, the cemented mine backfilling process involves the interaction of a number of complex mechanisms. To obtain the desired outcome of stress distribution, more research efforts should be dedicated to understanding the influence of each of mechanism via effective approaches. Most importantly, a coherent and rational procedure for mine backfilling analysis, which fully couples these mechanism and relevant safety issues, can pave the way for academic research and potential practical use in the mining industry.

Acknowledgement

The first author was financially supported by the China Scholarship Council (No. 201506420049).

References

[1] Y. Potvin and E. Thomas, *Handbook on Mine Fill*, Australian Centre for Geomechanics, Perth, 2005.
[2] M. Helinski, M. Fahey, and A. Fourie, Coupled two-dimensional finite element modelling of mine backfilling with cemented tailings, *Can. Geotech. J.*, 47(2010), No. 11, p. 1187.
[3] C.C. Qi, Big Data management in the mining industry, *Int. J. Miner. Metall. Mater.*, 27(2020), p. 131.
[4] E.F. Salmi, M. Nazem, and M. Karakus, The effect of rock mass gradual deterioration on the mechanism of post-mining subsidence over shallow abandoned coal mines, *Int. J. Rock Mech. Min. Sci.*, 91(2017), p. 59.
[5] T. Belem and M. Benzaazoua, Design, and application of underground mine paste backfill technology, *Geotech. Geol. Eng.*, 26(2008), No. 2, p. 147.
[6] N. Sivakugan, R.M. Rankine, K.J. Rankine, and K.S. Rankine, Geotechnical considerations in mine backfilling in Australia, *J. Cleaner Prod.*, 14(2006), No. 12-13, p. 1168.
[7] E. Yilmaz, T. Belem, and M. Benzaazoua, Study of physico-chemical and mechanical characteristics of consolidated and unconsolidated cemented paste backfills, *Gospod. Surowcami Miner.*, 29(2013), No. 1, p. 81.
[8] E. Yilmaz, A. Kesimal, and B. Erçikdi, The factors affecting strength and stability of paste backfill, *Yerbilimleri*, 28(2003), p. 155.
[9] E. Yilmaz, Stope depth effect on field behaviour and performance of cemented paste backfills, *Int. J. Min. Reclam. Environ.*, 32(2018), No. 4, p. 273.
[10] C.C. Qi, A. Fourie, and Q.S. Chen, Neural network and particle swarm optimization for predicting the unconfined compressive strength of cemented paste backfill, *Constr. Build. Mater.*, 159(2018), p. 473.
[11] C.C. Qi and A. Fourie, Cemented paste backfill for mineral tailings management: Review and future perspectives, *Miner. Eng.*, 144(2019), art. No. 106025.
[12] B.D. Thompson, W.F. Bawden, and M.W. Grabinsky, *In situ*

measurements of cemented paste backfill at the Cayeli Mine, *Can. Geotech. J.*, 49(2012), No. 7, p. 755.
[13] B.D. Thompson, M.W. Grabinsky, W.F. Bawden, and D.B. Counter, *In-situ* measurements of cemented paste backfill in long-hole stopes, [in] *ROCKENG09: Proceedings of the 3rd CANUS Rock Mechanics Symposium*, Toronto, 2009, p. 199.
[14] M. Aubertin, L. Li, S. Arnoldi, T. Belem, B. Bussière, M. Benzaazoua, and R. Simon, Interaction between backfill and rock mass in narrow stopes, *Soil Rock Am.*, 1(2003), p. 1157.
[15] M. Fahey, M. Helinski, and A. Fourie, Some aspects of the mechanics of arching in backfilled stopes, *Can. Geotech. J.*, 46(2009), No. 11, p. 1322.
[16] L. Li and M. Aubertin, Horizontal pressure on barricades for backfilled stopes. Part I: Fully drained conditions, *Can. Geotech. J.*, 46(2009), No. 1, p. 37.
[17] L. Cui and M. Fall, Multiphysics modeling of arching effects in fill mass, *Comput. Geotech.*, 83(2017), p. 114.
[18] H.A. Janssen, Versuche uber getreidedruck in silozellen, *Z. Ver. Dtsch. Ing.*, 39(1895), No. 35, p. 1045.
[19] A. Marston, *The Theory of External Loads on Closed Conduits in the Light of the Latest Experiments*, Iowa State College, Ames, 1930.
[20] K. Terzaghi, *Theoretical Soil Mechanics*, John Wiley and Sons. Inc., New York, 1965.
[21] C. Winch, *Geotechnical Characteristics and Stability of Paste Backfill at BHP Cannington Mine* [Dissertation], James Cook University, Townsville, 1999.
[22] T. Belem, A. Harvey, R. Simon, and M. Aubertin, Measurement of internal pressures of a gold mine pastefill during and after the stope backfilling, [in] *Proceedings of 5th International Symposium on Ground Support in Mining and Underground Construction*, Perth, 2004, p. 619.
[23] L. Li, M. Aubertin, and T. Belem, Formulation of a three dimensional analytical solution to evaluate stresses in backfilled vertical narrow openings, *Can. Geotech. J.*, 42(2005), No. 6, p. 1705.
[24] L. Li and M. Aubertin, Influence of water pressure on the stress state in stopes with cohesionless backfill, *Geotech. Geol. Eng.*, 27(2009), No. 1, art. No. 1.
[25] P. Rajeev, P.R. Sumanasekera, and N. Sivakugan, Average vertical stresses in underground mine stopes filled with granular backfills, *Geotech. Geol. Eng.*, 34(2016), No. 6, p. 2053.
[26] S.D. Widisinghe, *Stress Developments within a Backfilled Mine Stope and the Lateral Loading on the Barricade* [Dissertation], James Cook University, Townsville, 2014.
[27] J.E. Bowles, *Foundation Analysis and Design*, 5th ed., McGraw-Hill, New York, 1995.
[28] K. Pirapakaran and N. Sivakugan, A laboratory model to study arching within a hydraulic fill stope, *Geotech. Test. J.*, 30(2007), No. 6, p. 496.
[29] M.A. Sobhi, L. Li, and M. Aubertin, Numerical investigation of earth pressure coefficient along central line of backfilled stopes, *Can. Geotech. J.*, 54(2017), No. 1, p. 138.
[30] A.B. Fourie, M. Helinski, and M. Fahey, Using effective stress theory to characterize the behaviour of backfill, [in] *Proceedings of the Minefill Conference*, Perth, 2007, p. 27.
[31] L. Li and M. Aubertin, Numerical investigation of the stress state in inclined backfilled stopes, *Int. J. Geomech.*, 9(2009), No. 2, p. 52.
[32] R. Rankin, *Geotechnical Characterisation and Stability of Paste Fill Stopes at Cannington Mine* [Dissertation], James Cook University, Townsville, 2004.
[33] M. Helinski, *Mechanics of Mine Backfill* [Dissertation], University of Western Australia, Perth, 2007.
[34] R.E. Gibson, The progress of consolidation in a clay layer increasing in thickness with time, *Geotechnique*, 8(1958), No. 4, p. 171.
[35] E. Yilmaz, T. Belem, B. Bussière, M. Mbonimpa, and M. Benzaazoua, Curing time effect on consolidation behaviour of cemented paste backfill containing different cement types and contents, *Constr. Build. Mater.*, 75(2015), p. 99.
[36] T. Belem, O. El Aatar, B. Bussière, and M. Benzaazoua, Gravity-driven 1-D consolidation of cemented paste backfill in 3-m-high columns, *Innov. Infrastruct. Solut.*, 1(2016), No. 1, art. No. 37.
[37] M. Helinski, A. Fourie, M. Fahey, and M. Ismail, Assessment of the self-desiccation process in cemented mine backfills, *Can. Geotech. J.*, 44(2007), No. 10, p. 1148.
[38] L. Cui and M. Fall, Modeling of self-desiccation in a cemented backfill structure, *Int. J. Numer. Anal. Methods Geomech.*, 42(2018), No. 3, p. 558.
[39] H.Q. Jiang, M. Fall, and L. Cui, Yield stress of cemented paste backfill in sub-zero environments: Experimental results, *Miner. Eng.*, 92(2016), p. 141.
[40] J.M. Illston, J.M. Dinwoodie, and A.A. Smith, *Concrete, Timber and Metals. The Nature and Behaviour of Structural Materials*, Van Nostrand Reinhold, New York, 1979.
[41] E. Rastrup, The temperature function for heat of hydration in concrete, [in] *RELIM Symp.: Winter Concreting, Theory and Practice, Session B(II)*, Copenhagen, 1956.
[42] L. Cui and M. Fall, A coupled thermo–hydro-mechanical–chemical model for underground cemented tailings backfill, *Tunnelling Underground Space Technol.*, 50(2015), p. 396.
[43] T.C. Powers and T.L. Brownyard, Studies of the physical properties of hardened Portland cement paste, *J. Proc.*, 43(1946), No. 9, p. 101.
[44] M. Walske, *An Experimental Study of Cementing Paste Backfill* [Dissertation], University of Western Australia, Perth, 2014.
[45] R.E. Gibson, R.L. Schiffman, and K.W. Cargill, The theory of one-dimensional consolidation of saturated clays. II. Finite nonlinear consolidation of thick homogeneous layers, *Can. Geotech. J.*, 18(1981), No. 2, p. 280.
[46] M. Helinski, M. Fahey, and A. Fourie, Numerical modeling of cemented mine backfill deposition, *J. Geotech. Geoenviron. Eng.*, 133(2007), No. 10, p. 1308.
[47] M. Helinski, M. Fahey, and A. Fourie, Behavior of cemented paste backfill in two mine stopes: Measurements and modeling, *J. Geotech. Geoenviron. Eng.*, 137(2010), No. 2, p. 171.
[48] W.D. Carrier III, L.G. Bromwell, and F. Somogyi, Design capacity of slurried mineral waste ponds, *J. Geotech. Eng.*, 109(1983), No. 5, p. 699.
[49] O. Nasir and M. Fall, Modeling the heat development in hydrating CPB structures, *Comput. Geotech.*, 36(2009), No. 7, p. 1207.
[50] D. Wu, M. Fall, and S.J. Cai, Numerical modelling of thermally and hydraulically coupled processes in hydrating cemented tailings backfill columns, *Int. J. Min. Reclam. Environ.*, 28(2014), No. 3, p. 173.
[51] O. Nasir and M. Fall, Coupling binder hydration, temperature and compressive strength development of underground cemented paste backfill at early ages, *Tunnelling Underground Space Technol.*, 25(2010), No. 1, p. 9.
[52] L. Cui and M. Fall, Modeling of pressure on retaining structures for underground fill mass, *Tunnelling Underground Space Technol.*, 69(2017), p. 94.

[53] N. Falaknaz, M. Aubertin, and L. Li, Numerical investigation of the geomechanical response of adjacent backfilled stopes, *Can. Geotech. J.*, 52(2015), No. 10, p. 1507.
[54] A. Hasan, G. Suazo, J.P. Doherty, and A.B. Fourie, *In situ* measurements of cemented paste backfilling in an operating stope at Lanfranchi Mine, [in] *Proceedings of the Eleventh International Symposium on Mining with Backfill*, Perth, 2014, p. 20.,
[55] A. Hasan, G.H. Suazo, J. Doherty, and A. Fourie, In-stope measurements at two Western Australian mines, [in] *Proceedings of 17th Int. Seminar on Paste and Thickened Tailing Paste 2014*, Vancouver, 2014, p. 355.
[56] C.C. Qi and A. Fourie, Numerical investigation of the stress distribution in backfilled stopes considering creep behaviour of rock mass, *Rock Mech. Rock Eng.*, 52(2019), No. 9, p. 3353.
[57] X. Zhao, A. Fourie, and C.C. Qi, An analytical solution for evaluating the safety of an exposed face in a paste backfill stope incorporating the arching phenomenon, *Int. J. Miner. Metall. Mater.*, 26(2019), No. 10, p. 1206.
[58] L. Li and M. Aubertin, A modified solution to assess the required strength of exposed backfill in mine stopes, *Can. Geotech. J.*, 49(2012), No. 8, p. 994.
[59] R.J. Mitchell, R.S. Olsen, and J.D. Smith, Model studies on cemented tailings used in mine backfill, *Can. Geotech. J.*, 19(1982), No. 1, p. 14.
[60] S. Zou and N. Nadarajah, Optimizing backfill design for ground support and cost saving, [in] *Proceedings of Golden Rocks 2006: The 41st U.S. Symposium on Rock Mechanics (USRMS)*, Golden, Colorado, 2006.
[61] A.P.E. Dirige, R.L. McNearny, and D.S. Thompson, The effect of stope inclination and wall rock roughness on back-fill free face stability, [in] *Rock Engineering in Difficult Conditions: Proceedings of the 3rd Canada–US Rock Mechanics Symposium*, Toronto, 2009.
[62] A.P.E. Dirige and E. De Souza, Engineering design of backfill systems in adjacent pillar mining, [in] *Proceedings of the 42nd U.S. Rock Mechanics Symposium (USRMS)*, Alexandria, 2008.
[63] N.R. Morgenstern and V.E. Price, A numerical method for solving the equations of stability of general slip surfaces, *Comput. J.*, 9(1967), No. 4, p. 388.
[64] Z.Y. Chen and N.R. Morgenstern, Extensions to the generalized method of slices for stability analysis, *Can. Geotech. J.*, 20(1983), No. 1, p. 104.
[65] H.Z. Jiao, S.F. Wang, A.X. Wu, H.M. Shen, and J.D. Wang, Cementitious property of $NaAlO_2$-activated Ge slag as cement supplement, *Int. J. Miner. Metall. Mater.*, 26(2019), No. 12, p. 1594.
[66] Y.Y. Tan, X. Yu, D. Elmo, L.H. Xu, and W.D. Song, Experimental study on dynamic mechanical property of cemented tailings backfill under SHPB impact loading, *Int. J. Miner. Metall. Mater.*, 26(2019), No. 4, p. 404.
[67] N.J.F. Koupouli, T. Belem, P. Rivard, and H. Effenguet, Direct shear tests on cemented paste backfill–rock wall and cemented paste backfill–backfill interfaces, *J. Rock Mech. Geotech. Eng.*, 8(2016), No. 4, p. 472.
[68] O. Nasir and M. Fall, Shear behaviour of cemented pastefill–rock interfaces, *Eng. Geol.*, 101(2008), No. 3-4, p. 146.
[69] M. Fall and O. Nasir, Mechanical behaviour of the interface between cemented tailings backfill and retaining structures under shear loads, *Geotech. Geol. Eng.*, 28(2010), No. 6, p. 779.
[70] K. Fang and M. Fall, Shear behavior of the interface between rock and cemented backfill: Effect of curing stress, drainage condition and backfilling rate, *Rock Mech. Rock Eng.*, 53(2020), p. 325.
[71] T. Belem, M. Benzaazoua, B. Bussière, and A.M. Dagenais, Effects of settlement and drainage on strength development within mine paste backfill, [in] *Proceedings of Tailings and Mine Waste '02*, Balkema, Rotterdam, 2002, p. 139.
[72] K.A. Le Roux, W.F. Bawden, and M.W.F. Grabinsky, Assessing the interaction between hydration rate and fill rate for a cemented paste backfill, [in] *Proceedings of the 55th Canadian Geotechnical and 3rd Joint IAH-CNC Groundwater Specialty Conference*, Niagara Falls, Ontario, 2002, p. 427.
[73] M. Fahey, M. Helinski, and A. Fourie, Development of specimen curing procedures that account for the influence of effective stress during curing on the strength of cemented mine backfill, *Geotech. Geol. Eng.*, 29(2011), No. 5, p. 709.
[74] M.B. Revell and D.P. Sainsbury, Paste bulkhead failures, [in] *Proceedings of International Symposium of MineFill07*, Montreal, 2007.
[75] M.B. Revell and D.P. Sainsbury, Advancing paste fill bulkhead design using numerical modeling, [in] *Proceedings of International Symposium of MineFill07*, Montreal, 2007.
[76] N. Sivakugan, K. Rankine, and R. Rankine, Permeability of hydraulic fills and barricade bricks, *Geotech. Geol. Eng.*, 24(2006), No. 3, p. 661.
[77] J. Li, J.V. Ferreira, and T. Le Lievre, Transition from discontinuous to continuous paste filling at Cannington Mine, [in] *Proceedings of the 11th International Symposium on Mining with Backill*, Preth, 2014, p. 381.
[78] R.L. Veenstra, *A Design Procedure for Determining the In Situ Stresses of Early Age Cemented Paste Backfill* [Dissertation], University of Toronto, Toronto, 2013.
[79] L. Li and M. Aubertin, Horizontal pressure on barricades for backfilled stopes. Part II: Submerged conditions, *Can. Geotech. J.*, 46(2009), No. 1, p. 47.
[80] A. Cheung, *Influence of Rock Boundary Conditions on Behaviour of Arched and Flat Cemented Paste Backfill Barricade Walls* [Dissertation], University of Toronto, Toronto, 2012.
[81] S. Ghazi, *Modeling of an Underground Mine Backfill Barricade* [Dissertation], University of Toronto, Toronto, 2011.